Geomechanics and Engineering, *Vol. 11*, *No. 1* (*2016*) *161-175*
DOI: http://dx.doi.org/10.12989/gae.2016.11.1.161

Experimental study on deformation and strength property of compacted loess

Yuan Mei [*1], Chang-Ming Hu [1], Yi-Li Yuan [1], Xue-Yan Wang [1,2] and Nan Zhao [1]

[1] *College of Civil Engineering, Xi'an University of Architecture and Technology, Xi'an, China*
[2] *College of Environmental and Chemical Engineering, Xi'an Polytechnic University, Xi'an, China*

(*Received January 30, 2015, Revised April 05, 2016, Accepted April 17, 2016*)

Abstract. A series of experimental studies are conducted on the deformation and shear strength property of compacted loess. The results reveal that the relationships of both the initial moisture content (w) and the initial degree of compaction (K) of compacted loess with cohesion (w) and the angle of internal friction (φ) are linear. The relationship between the secant modulus (E_{soi}) and K is also linear. The relationship between E_{soi} and w can be fitted well by a second-order polynomial. Further, when the influences of w and K are ignored, the relationship between the confined compression strain (ε) and vertical pressure (p) can be expressed by a formula. A correction formula for the deformation of compacted loess caused by a change in w and K is derived on the basis of the study results.

Keywords: compacted loess; shear strength; deformation property; deformation correction formula

1. Introduction

Loess is widely distributed around the world. From a geotechnical point of view, the most significant characteristics of loess are its collapsibility, sensitivity to moisture content, structural strength, and vertical joints (Liang *et al*. 2015). Loess is well known worldwide for its superior behavior and is widely used as filling material in engineering projects (Daehyeon and Kang 2013). However, it is known that in construction projects, foundation subsidence often occurs in the collapsible loess region owing to the presence of water and the complex composition of loess particles, large pores, and a loose structure (Wang *et al*. 2014c).

The shear strength of loess is one of the important mechanical properties of construction materials (Qian *et al*. 2014, Bowders *et al*. 2000). Because of the distinctive physical and mechanical properties of loess, its shear strength property and deformation mechanism have recently attracted research attention (Acharya *et al*. 2011, Zhang *et al*. 2013, Haeri *et al*. 2014, 2016). Many researchers have conducted a considerable amount of useful research on this topic.

With the aim of studying the deformation property of large-thickness self-weight collapsible loess and for understanding the moisture migration law and matrix suction characteristics, Wang *et al*. (2014c) performed a 40-m-diameter soaking test in the field by using self-weight collapsible loess with a thickness of 36.5 m. The collapse behavior of soil in a Brazilian region affected by a rising water table also has been studied extensively, and the results of such research indicate that a

*Corresponding author, Ph.D., E-mail: my0326@126.com

 ISSN: 2005-307X (Print), 2092-6219 (Online)

continuous process of suction reduction diminishes the soil shear strength and results in the soil reaching new equilibrium conditions (Vilar and Rodrigues 2011). Moreover, research by Zhuang and Peng (2014) has led to the conclusion that with an increase in water content, the paleosol layer strength decreases more sharply than does the loess strength. According to Daehyeon and Kang (2013), the collapsible potential of loess can be significantly improved by compacting it well when it is used as a filling material. Moreover, a new method for the calculation of comprehensive shear parameters has been proposed (Liang *et al*. 2015).

Several fundamental achievements have been made in research on the deformation and strength of compacted soil (Rahardjo *et al*. 2009, Dzagov 2009, Luo *et al*. 2014). Chen and Sha (2010) analyzed the deformation property of compacted loess. Further, Wang *et al*. (2010) performed a qualitative examination to study the general trend of the variation of cohesion and the angle of internal friction of compacted loess-like silt with a change in the dry density and moisture content. Luo (2011) evaluated the effects of moisture conditions on the shear strength of compacted soil. Furthermore, Shen *et al*. (2009) demonstrated that cohesion and the angle of internal friction of unsaturated soils decrease linearly with an increase in moisture content and that cohesion increases exponentially with an increase in the dry density. Cheng *et al*. (2008) investigated the influence of dry density and moisture content on the strength parameters of loess. Chen and Sha (2009) discussed the relationship between the cohesion and moisture content of compacted soil samples whose moisture content is around the optimum moisture content. Li and Miao (2009) estimated the water sensitivity of the shear strength and stress-deformation mechanism of loess under different deposition times and moisture conditions. Furthermore, several researchers discussed the influence of water content or structural strength on the shear strength of loess (He 2008, Fang *et al*. 2011) and on its deformation behaviors and creep characteristics (Wu *et al*. 2012, Tang *et al*. 2014). In addition, extensive works were conducted on important problems pertaining to loess, and many important conclusions were drawn (Wang *et al*. 2014a, b, Muñoz-Castelblanco *et al*. 2011, 2012).

The structure and physical mechanics of loess change when it is compacted. For example, soils having moisture contents lower than the optimum moisture content are characterized by higher strength and lower confined compressibility (at a low stress level) under a certain compaction energy and dry density. When the moisture content of unsaturated compacted clay is lower than the optimum moisture content, its cohesion also decreases with a decrease in the moisture content. Therefore, research results of normal loess or undisturbed loess cannot be used in the strength analysis and deformation calculation problem of loess. Therefore, a systematic study of the strength and deformation property of compacted loess is required. In the present work, the relationships of the initial degree of compaction and initial moisture content with shear strength parameters and confined compression deformation are studied through compact and direct shear tests. Additionally, a correction formula for the deformation of compacted loess under changing moisture content and degree of compaction is derived. The results of this research are expected to be useful in analyzing and calculating the deformation of foundation filled by compacted loess.

2. Material

The test soil samples were collected from Lvliang in China which is typical Malan loess. The soil sample used in the test is shown in Fig. 1. The grain size composition of compacted loess is presented in Table 1.

Fig. 1 Soil sample used in tests

Table 1 Grain size composition of loess used in tests

Grain composition	Grain diameter /μm	Content /%
Fine sand	75~250	0.7
Silty sand	50~75	16.6
Coarse grain silt	10~50	58.0
Fine grained silt	5~10	8.9
Clay particle	< 5	15.8

In order to determine the maximum dry density ρ_{dmax} and optimum moisture content w_{op} of the loess used in the tests, six heavy compaction tests were performed. Fig. 2 shows the curve of the relationship between the dry density ρ and the initial moisture content w obtained from the tests.

The test results show that with an increase in w, ρ first increases and then decreases. When w increases to w_{op} and continues to increase further, ρ decreases rapidly, as is the case with clay, which demonstrates that loess is sensitive to moisture content. w_{op} of the soil samples ranges from 12.3% to 14.2%, and ρ_{dmax} ranges from 1.85 g/cm^3 to 1.89 g/cm^3.

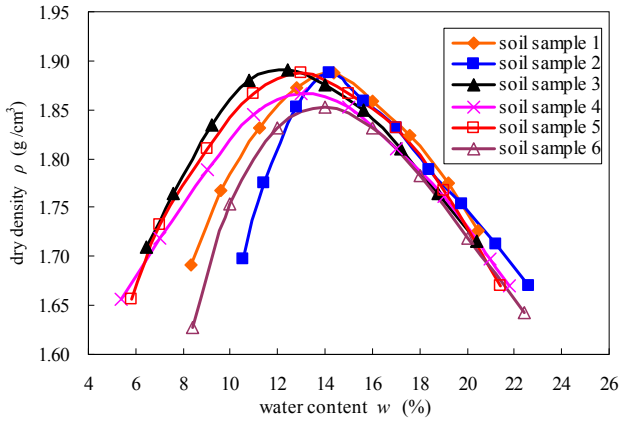

Fig. 2 Curve of relationship between dry density (ρ) and initial moisture content (w)

It can be seen from Fig. 2 that ρ first increases and then decreases with a change in w. This behavior of loess can be explained using the principle of effective stress (Olson 1998, Vahedifard *et al*. 2016). Under a small moisture content, the cohesion c of soil is strong and ρ is low. Moreover, the arrangement direction of soil particles is irregular and the soil has a lamellar structure. In the process of increase in the moisture content to the optimal value, gas is more likely to be discharged from the soil being compacted. Simultaneously, c of the soil decreases, which causes the occurrence of a larger displacement of particles. Further, because of the lubrication between the soil particles, the density of soil is more likely to increases. At this time, ρ clearly increases with an increase in w. When w exceeds the optimal value, the additional pore water pressure will offset a considerable amount of external force. The confining gas inside the soil shrinks under external pressure and thus offsets part of the compaction effect. In addition, the decrease in the sidewall friction force of soil results in effective work because of the displacement of the soil particles. In this situation, the compaction effect worsens and the compaction dry density correspondingly decreases.

3. Test results

Most of the compacted loess is unsaturated, and its w and initial degree of compaction K can be measured easily. Direct research on the change in the shear strength of loess with a change in w and K is approximate and empirical. However, this is a practical method, and avoids measuring the suction, which is difficult to realize. For a particular type of soil, w and K are, no doubt, the most

Table 2 Initial moisture content (w) and initial degree of compaction (K) of soil samples

K_i /%	w_{ij} /%			
$K_1 = 90\%$	$w_{11} = 11.2\%$	$K_1 = 90\%$	$w_{11} = 11.2\%$	$K_1 = 90\%$
$K_2 = 93\%$	$w_{21} = 11.2\%$	$K_2 = 93\%$	$w_{21} = 11.2\%$	$K_2 = 93\%$
$K_3 = 95\%$	$w_{31} = 11.2\%$	$K_3 = 95\%$	$w_{31} = 11.2\%$	$K_3 = 95\%$
$K_4 = 98\%$	$w_{41} = 11.2\%$	$K_4 = 98\%$	$w_{41} = 11.2\%$	$K_4 = 98\%$

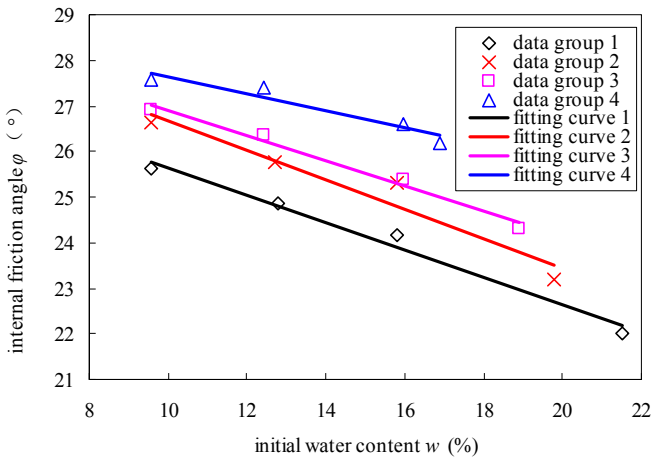

Fig. 3 Curve of relationship between initial moisture content (w) and angle of internal friction (φ)

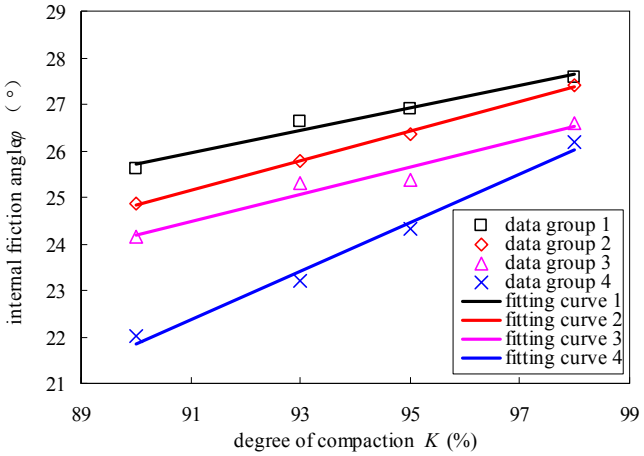

Fig. 4 Curve of relationship between initial degree of compaction (K) and angle of internal friction (φ)

important factors for the determination of the soil's shear strength. Each sample of the test should be created to have the same w and different K as much as possible. The initial moisture content (w_{ij}) and initial degree of compaction (K_i) of the soil samples are presented in Table 2.

3.1 Relationship of φ with w and K

Figs. 3 and 4, respectively, show the curves of the relationship between φ and w and of the relationship between φ and K obtained from a series of direct shear tests. Tables 3 and 4, respectively, present analyses of the relationship between φ and w and of the relationship between φ and K (i, j = 1, 2, 3, or 4).

It can be seen from Figs. 3 and 4 that under a certain K, the φ value of the soil sample decreases with an increase in the w value. Furthermore, the smaller the value of K, the stronger is the

Table 3 Analysis of relationship between angle of internal friction (φ) and initial moisture content (w)

Date group	K	w	Fitting function	R^2
1	K_1	w_{1j}	$\varphi_1 = -0.3017w + 28.658$	0.9828
2	K_2	w_{2j}	$\varphi_2 = -0.3256w + 29.938$	0.9410
3	K_3	w_{3j}	$\varphi_3 = -0.2776w + 29.688$	0.9831
4	K_4	w_{4j}	$\varphi_4 = -0.1851w + 29.483$	0.9229

Table 4 Analysis of relationship between angle of internal friction (φ) and initial degree of compaction (K)

Date group	K	w	Fitting function	R^2
1	K_i	w_{i1}	$\varphi_1 = 0.2382K + 4.2859$	0.9712
2	K_i	w_{i2}	$\varphi_2 = 0.3174K - 3.7312$	0.9990
3	K_i	w_{i3}	$\varphi_3 = 0.2906K - 1.9528$	0.9549
4	K_i	w_{i4}	$\varphi_4 = 0.5247K - 25.392$	0.9861

influence of w on φ. Moreover, under a certain value of w, the φ value of the soil sample increases with an increase in the K value. In addition, the higher the w value, the stronger is the influence of K on φ. With an increase in K and a decrease in w, both c and φ increase. Nevertheless, the influences of w and K on cohesion are much stronger than those on φ are. Both these relationships are linear.

It can be seen from the data depicted above that φ decreases with an increase in the moisture content irrespective of the K value. This is because the water present in the soil is mainly in the form of a bound water membrane around the soil particles. The water molecules in strongly bound water membrane cannot move, whereas those in weakly bound membrane can move along the surface of the soil particles and thus provide a lubrication effect between the soil particles. The value of φ is a comprehensive reflection of the friction condition between the soil particles. The thickness of the weakly bound water membrane increases with an increase in the moisture content. The friction effect between the soil particles decreases in the presence of shearing force, which results in a decrease in φ with an increase in w.

It is obvious that φ increases with increasing degree of compaction. This is attributed to the following three reasons. First, the degree of tightness between the soil particles increases with an increase in the degree of compaction, which, in turn, enhances the interaction between the soil particles and the water membrane. Second, the increase in the degree of compaction causes a decrease in the void ratio. The water molecules are in the form of a strongly bound water membrane and so they cannot move, which results in an increase in the soil intensity. Third, the spacing between the soil particles decreases gradually with an increase in the degree of compaction. The thickness of the bound water membrane decreases and part of the water is converted into free water, which leads to a reduction in the lubrication effect and thus an increase in φ.

3.2 Relationship of c with w and K

Figs. 5 and 6, respectively, show the curves of the relationship between c and w and of the relationship between c and K obtained from the tests. Tables 5 and 6, respectively, present analyses of the relationship between c and w and of the relationship between c and K (i, j = 1, 2, 3, or 4).

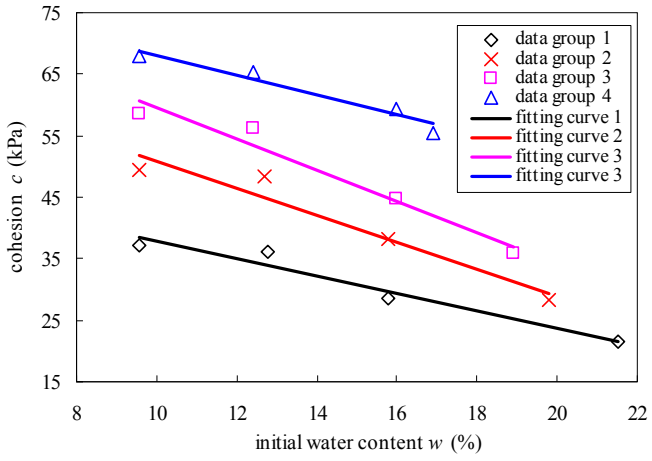

Fig. 5 Curve of relationship between initial moisture content (w) and cohesion (c)

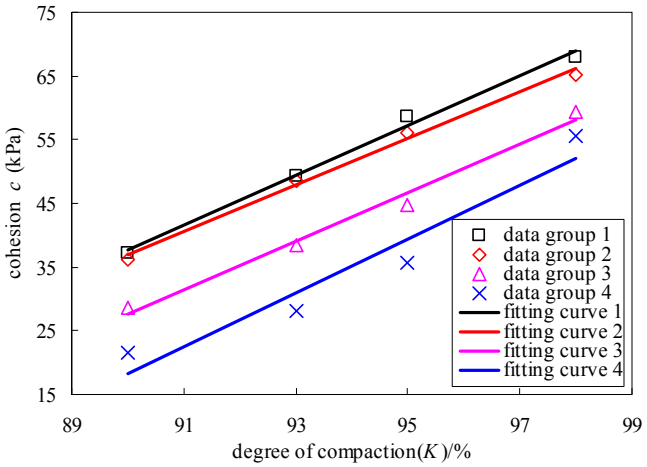

Fig. 6 Curve of relationship between initial degree of compaction (K) and cohesion (c)

Table 5 Analysis of relationship between cohesion (c) and initial moisture content (w)

Date group	K	w	Fitting function	R^2
1	K_i	w_{1j}	$c_1 = -1.4102w + 51.885$	0.9566
2	K_i	w_{2j}	$c_2 = -2.1954w + 72.856$	0.9313
3	K_i	w_{3j}	$c_3 = -2.5532w + 85.103$	0.9625
4	K_i	w_{4j}	$c_4 = -1.6554w + 86.022$	0.9503

Table 6 Analysis of relationship between cohesion (c) and initial degree of compaction (K)

Date group	K	w	Fitting function	R^2
1	K_i	w_{i1}	$c_1 = 3.8915K - 312.50$	0.9938
2	K_i	w_{i2}	$c_2 = 3.6559K - 292.17$	0.9939
3	K_i	w_{i3}	$c_3 = 3.8056K - 314.95$	0.9851
4	K_i	w_{i4}	$c_4 = 4.2312K - 362.49$	0.9337

It can be seen from Fig. 5 that c decreases with an increase in w under a certain K. The reason for this may be the increase in the water molecule in weakly bound water film of the soil with an increase in w. This leads to a stronger lubrication effect between soil grains and a weaker occlusion effect between them owing to the water pressure caused by free water; and as a result, the cohesion reduces. Moreover, the smaller the K value, the greater is the influence of w on c. When w is smaller than w_{op}, the influence of w on c is small, and vice versa.

Furthermore, Fig. 6 shows that c increases with an increase in K under a certain w. This is because the higher the K value, the tighter the soil grains become, which finally leads to a stronger occlusion effect between soil grains. Moreover, the variation tendency of c with an increase in K is almost the same under different w values. This indicates that under different w values, the increase in c caused by the increase in K is not restricted by w.

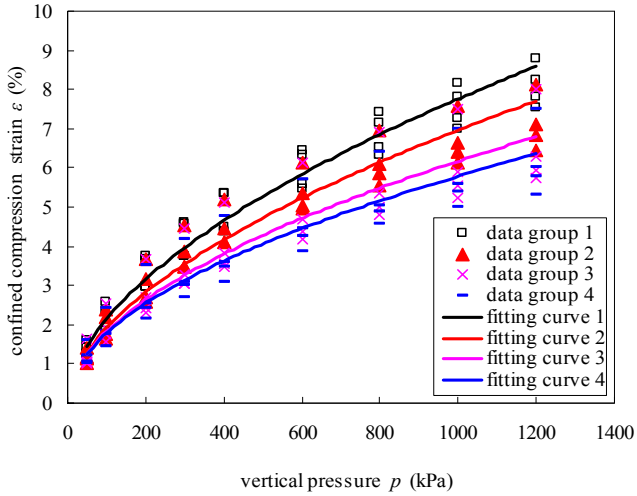

Fig. 7 Curve of relationship between confined compression strain (ε) and vertical pressure (p)

3.3 Relationship of ε with p

In order to determine the influence of K and w on the compressive deformation of compacted loess, a compression test with different K and w values (as listed in Table 2) was performed. Compression levels considered in the test were 50 kPa, 100 kPa, 200 kPa, 300 kPa, 400 kPa, 600 kPa, 800 kPa, 1000 kPa, and 1200 kPa. The stabilized reference permits deformation within 0.01 mm at each level. The curve of the relationship between the confined compressive strain (ε) and the vertical pressure (p) obtained from the test is shown in Fig. 7.

It can be seen from Fig. 7 that under a certain w, the higher the K value, the smaller is the ε value. Furthermore, ε increases more rapidly with an increase in p and w. This indicates that the influence of K on compressive deformation increases with an increase in w.

Furthermore, vertical analysis shows that under a certain K, the higher the w value, the larger is the ε value. Additionally, ε increases more slowly with an increase in p and K. This indicates that the influence of w on compressive deformation decreases with an increase in K. Therefore, increasing K is an effective way to control the deformation of foundation filled by compacted loess.

Judging from Fig. 7, the curve of the relationship between ε and p approximates to a power function curve. Therefore, a power function is used to fit this relationship. Analysis of the fitting function is presented in Table 7 (j = 1, 2, 3, or 4).

According to Table 7, the relationship between ε and p can be expressed by the following formula

Table 7 Analysis of relationship between ε and p

Date group	K	w	Fitting function	R^2
1	K_1	w_{1j}	$\varepsilon_1 = 0.1645p^{0.5580}$	0.9683
2	K_2	w_{2j}	$\varepsilon_2 = 0.1458p^{0.5596}$	0.9541
3	K_3	w_{3j}	$\varepsilon_3 = 0.1605p^{0.5283}$	0.9122
4	K_4	w_{3j}	$\varepsilon_4 = 0.1706p^{0.5101}$	0.9145

$$\varepsilon = kp^n \tag{1}$$

In Eq. (1), k and n are constants that can be obtained from tests.

3.4 Relationship of secant modulus (E_{soi}) with K

The size of the test data was extremely large, therefore, in order to simplify the analysis, with the consideration that soils whose w is lower than w_{op} are commonly used in filling engineering, compaction test results for 100 kPa, 200 kPa, 400 kPa, and 800 kPa under w_{op} were used to analyze the relationship between ε and p. The test results are shown in Fig. 8. Analysis of the fitting function of the relationship between K and E_{soi} is presented in Table 8 (j = 1, 2, 3, or 4).

It can be seen from Fig. 8 that the influence of w on E_{soi} is significant when K is between 93% and 95%. In this range, the rate of change in E_{soi} decreases with an increase in w. It can also be clearly seen that the relationships between E_{soi} and K under each w value are linear.

Table 8 Analysis of relationship between initial degree of compaction (K) and secant modulus (E_{soi})

Date group	p /kPa	w	Fitting function	R^2
1	*50*	w_{i2}	$E_{soi1} = 87.941K - 3766.5$	0.8521
2	100	w_{i2}	$E_{soi2} = 40.69K + 1795.4$	0.9095
3	200	w_{i2}	$E_{soi3} = 188.25K - 10041$	0.9117
4	300	w_{i2}	$E_{soi4} = 271.03\ K - 16363$	0.8817
5	400	w_{i2}	$E_{soi5} = 336.51K - 21276$	0.9130
6	600	w_{i2}	$E_{soi6} = 439.92\ K - 28741$	0.9152
7	800	w_{i2}	$E_{soi7} = 551.71K - 37280$	0.9140
8	1000	w_{i2}	$E_{soi8} = 636.08\ K - 43320$	0.9192
9	1200	w_{i2}	$E_{soi9} = 707.04\ K - 48033$	0.9204

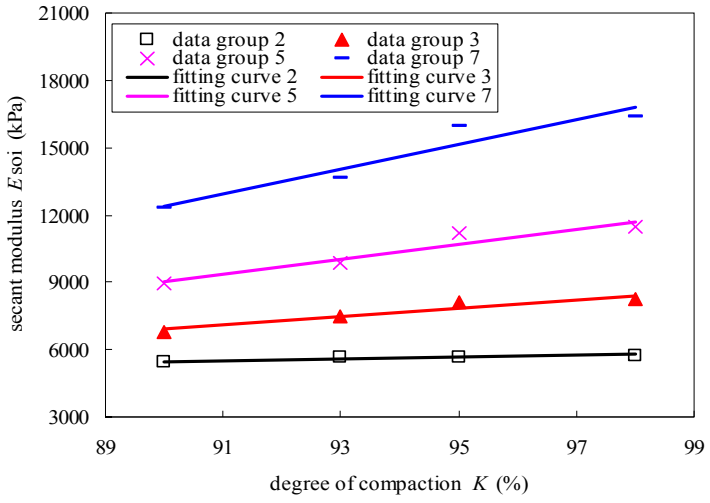

Fig. 8 Curve of relationship between initial degree of compaction (K) and secant modulus (E_{soi})

According to Table 8, the relationship between E_{soi} and K of compacted loess can be described as follows

$$E_{soi}^{K} = \alpha K_i + \beta \tag{2}$$

In Eq. (2), α and β are constants that can be obtained from tests.

3.5 Relationship of E_{soi} with w

Analysis of the test data shows that there is no appropriate formula to directly express the relationship between E_{soi} and w of the soil sample. However, further analysis revealed that the numerical relationship between E_{soi} and the reciprocal of w, denoted as ξ, can be fitted well by a second-order polynomial, as shown in Fig. 9 (because of space constraints, only some of the test data are shown).

Analysis of the fitting function of the relationship between E_{soi} and ξ is presented in Table 9 ($K = K_2$).

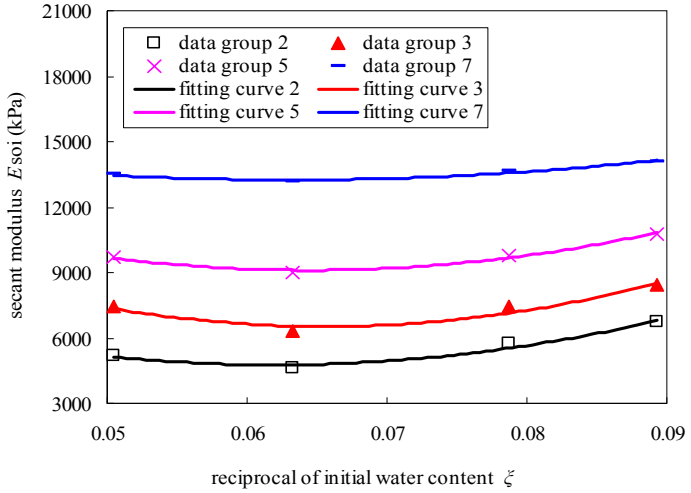

Fig. 9 Curve of relationship between secant modulus (E_{soi}) and reciprocal of w (ξ)

Table 9 Analysis of relationship between secant modulus (E_{soi}) and reciprocal of w (ξ)

Date group	P /kPa	K	Fitting function	R^2
1	50	K_2	$E_{soi1} = 4E+06\xi^2 - 520951\xi + 22310$	0.9962
2	100	K_2	$E_{soi2} = 4E+06\xi^2 - 472308\xi + 22020$	0.9293
3	200	K_2	$E_{soi3} = 3E+06\xi^2 - 338146\xi + 15238$	0.9694
4	300	K_2	$E_{soi4} = 1E+06\xi^2 - 142039\xi + 11313$	0.9991
5	400	K_2	$E_{soi5} = 3E+06\xi^2 - 361500\xi + 20754$	0.9843
6	600	K_2	$E_{soi6} = 763357\xi^2 - 56419\xi + 11677$	0.9960
7	800	K_2	$E_{soi7} = 1E+06\xi^2 - 165357\xi + 18462$	0.9513
8	1000	K_2	$E_{soi8} = 1E+06\xi^2 - 158764\xi + 19795$	0.9926
9	1200	K_2	$E_{soi9} = 3E+06\xi^2 - 336465\xi + 28288$	0.9386

The tendency formula is derived on the basis of the data in Table 9

$$E_{soi}^{w} = a\xi^2 + b\xi + c \tag{3}$$

In Eq. (3), a, b, and c are constants, and ξ is the reciprocal of w.

It can be seen from the test results that ξ of the soil sample decreases with an increase in w under each K. Furthermore, the influence of K on the development of free water pressure is significant only when the degree of saturation reaches a certain level. This phenomenon can be explained by the following interaction effect between soil grains and water: when K is low, pores in the soil are large, thereby making the soil grains rather loose and causing free water and air in the soil to discharge easily. Therefore, the influence of w on the soil strength is quite weak. In contrast, when K is high, pores in the soil are small, thereby making the soil grains tightly contacted. Removal of free water and air in the soil is difficult, and sufficient free water pressure develops. Therefore, a change in w will not greatly change the water pressure in the soil. Under a certain K, when w increases both the amount of free water and the number of water molecules that exist in the form of weakly bound water film increase. When the free water pressure reaches a certain level, the change in the water pressure caused by the change in w will be slower. The influence of w on the soil strength will therefore reduce.

4. Discussion

Under pressure p_j, when w, K of the soil samples changes from w_1, K_1 to w_2, K_2, E_{soi} of the soil sample changes from E^*_{soi1} to E^*_{soi2} (where "*" represents w or K) and ε changes from ε^*_{i1} to ε^*_{i2}. If the initial height of the soil samples is h_0, the deformation of the sample under pressure p_j is given as

$$\begin{cases} \Delta h_{i1} = \varepsilon^*_{i1} h_0 \\ \Delta h_{i2} = \varepsilon^*_{i2} h_0 \end{cases} \tag{4}$$

By the definition of E_{soi}, i.e., $E_{soi} = p_i/\varepsilon_i$, deformation of the sample under pressure p_j is

$$\Delta H = \left|\Delta h_{i2} - \Delta h_{i1}\right| = p_i h_0 \left| \frac{1}{E^*_{soi2}} - \frac{1}{E^*_{soi1}} \right| \tag{5}$$

Through substitution of Eqs. (2) and (3) into Eq. (5) and use of the definition of the coefficient of deformation of the soil sample, i.e., $\Delta\delta_{il,2} = \Delta H/h_0$, the coefficient of deformation of the soil sample when w, K of the soil sample changes from w_1, K_1 to w_2, K_2 is defined as

$$\begin{cases} \Delta\delta^{w}_{i1,2} = p_i \dfrac{\left|a(\xi_1^2 - \xi_2^2) + b(\xi_1 - \xi_2)\right|}{(a\xi_1^2 + b\xi_1 + c)(a\xi_2^2 + b\xi_2 + c)} \\ \Delta\delta^{K}_{i1,2} = p_i \dfrac{\alpha(K_2 - K_1)}{(\alpha K_1 + \beta)(\alpha K_2 + \beta)} \end{cases} \tag{6}$$

Therefore, when w or K of an S^*-thick soil layer is changed, the revised deformation ΔH^* will be

$$\begin{cases} \Delta H^{w} = p_i S^{w} \dfrac{\left|a(\xi_1^2 - \xi_2^2) + b(\xi_1 - \xi_2)\right|}{(a\xi_1^2 + b\xi_1 + c)(a\xi_2^2 + b\xi_2 + c)} \\ \Delta H^{K} = p_i S^{K} \dfrac{\alpha(K_2 - K_1)}{(\alpha K_1 + \beta)(\alpha K_2 + \beta)} \end{cases} \tag{7}$$

In order to verify the validity of Eq. (7), a series of numerical analyses are performed, and the results are compared with the calculation results obtained using Eq. (7). The material considered for the numerical model is homogeneous compacted loess. The length, width, and height of the model are 300 m, 300 m, and 10 m, respectively. In order to simulate the earth pressure of the upper soil, a uniform distributed load with a size of 100 m × 100 m and magnitude of 300 kPa is applied to the model. Because of the symmetry of the model, a 1/4 model is established, as shown in Fig. 10(a). It is assumed that when w of the soil is 12.4%, K increases gradually from 89% to 99%. When K is 93%, w increases gradually from 9% to 19%. The soil constitutive model is an ideal elastic–plastic model. The shear strength of the soil is determined from the test results described above. Representative calculation results are shown in Fig. 10(b).

A comparative analysis between the numerical calculation results and the results calculated using Eq. (7) is shown in Fig. 11.

It can be seen from Fig. 11 that the results calculated using Eq. (7) are close to the numerical calculation results. The error is small, and it decreases with an increase in the change in K and w, which indicates that the results calculated using Eq. (7) are reasonable.

In the construction process of high embankments at an airport and a roadbed, construction process of large public facilities, and other projects in a gully region, the load of the lower soil layer increases gradually, and K also increases gradually because of compressive deformation. The permeation of surface water, evaporation, and moisture migration also result in changes in w. Thus, in the calculation of the deformation of filling foundation pit during and after the construction period, the influences of K and w can be ignored at first, and Eq. (1) can be used to calculate the deformation of the filling body; subsequently, the results can be updated by calculating the coefficient of deformation when w, K changes from w_1, K_1 to w_2, K_2 under pressure p_j through Eq. (7).

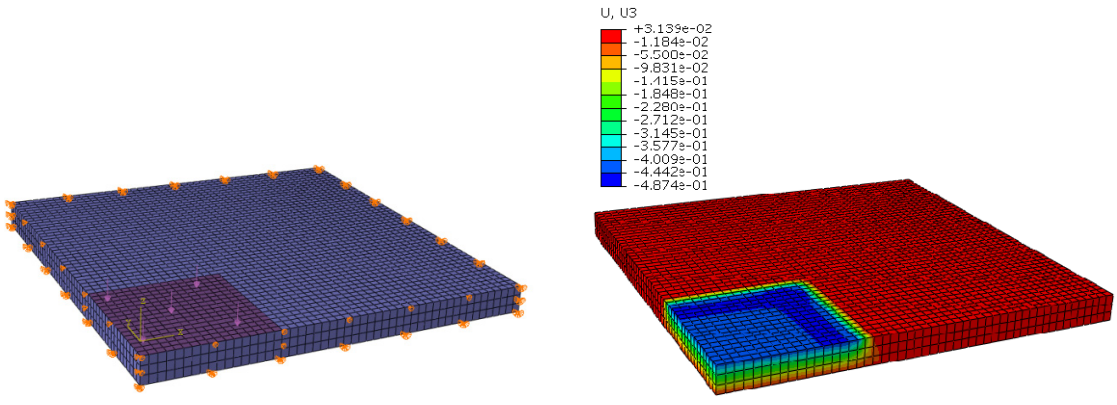

(a) (b)

Fig. 10 (a) Numerical analysis model; (b) Representative calculation results

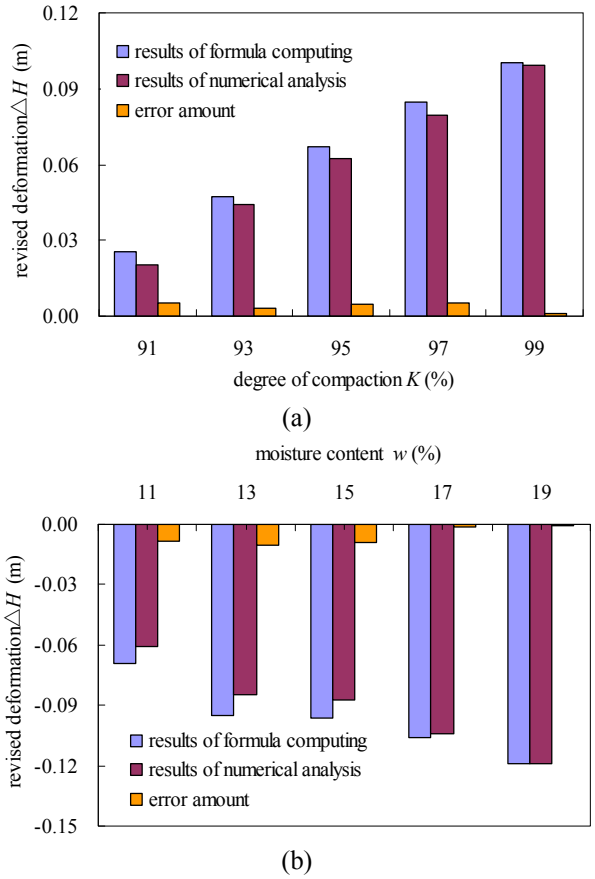

Fig. 11 (a) Comparative analysis between numerical calculation results and formula calculation results (under varying initial degree of compaction (K)); (b) Comparative analysis between numerical calculation results and formula calculation results (under varying initial moisture content (w))

5. Conclusions

In this study, a series of experimental researches were conducted on the deformation and shear strength property of compacted loess, and the following conclusions were drawn.

- With an increase in the initial degree of compaction (K) and a decrease in the initial moisture content (w), both the cohesion (c) and the angle of internal friction (φ) of loess increase, but the influences of w and K on c are much stronger than those on φ are. Both these relationships are linear.
- The higher the K value, the smaller is the confined compression strain (ε). Additionally, the influence of K on compressive deformation increases with an increase in w. The higher the w value, the larger is ε. Further, the influence of w on compressive deformation decreases with an increase in K. If the influences of K and w are ignored, the relationship between ε and the vertical pressure (p) can be described by the power function $\varepsilon = kp^n$.
- When K and w change, the deformation of foundation filled with compacted loess can be updated using Eq. (7) derived in this study.

Acknowledgments

This work was supported by the National Natural Science Foundation of China (No. 51408463), Special Research Project of Education Department of Shaanxi Provincial Government (Grant No. 15JK1413), Scientific Plan of Xi'an University of Architecture and Technology (No. RC1375), and Scientific Project of Xi'an University of Architecture and Technology (No. QN1409).

References

Acharya, G., Cochrane, T., Davies, T. and Bowman, E. (2011), "Quantifying and modeling post-failure sediment yields from laboratory-scale soil erosion and shallow landslide experiments with silty loess", *Geomorphology*, **129**(1-2), 49-58.

Bowders, J.J., Loehr, J.E. and Owen, J.W. (2000), "Shear behavior of compacted silty loess", *Geotechnical Special Publication*, **99**, 235-246.

Chen, K.S. and Sha, A.M. (2009), "Study on strength characteristic for loess subgrade filter of Yumenkou-Yanliang highway", *Hydrogeol. Eng. Geol.*, **36**(5), 44-48.

Chen, K.S. and Sha, A.M. (2010), "Study of deformation characteristic of compacted loess", *Rock Soil Mech.*, **31**(4), 1023-1030.

Cheng, H.T., Liu, B.J. and Xie, Y.L. (2008), "Stress-strain-time behavior of compacted loess", *J. Chang'an Univ.* (*Natural Science Edition*), **28**(1), 6-9.

Daehyeon, K. and Kang, S.S. (2013), "Engineering properties of compacted loesses as construction materials", *J. Civil Eng.*, **17**(2), 335-341.

Dzagov, A.M. (2009), "Determination of characteristics of the proneness of loess soils to slump-type settlement", *Soil Mech. Found. Eng.*, **46**(6), 260-268.

Fang, X.W., Shen, C.N., Chen, Z.H. and Zhang, W. (2011), "Triaxial wetting tests of intact Q_2 loess by computed tomography", *China Civil Eng. J.*, **44**(10), 98-106.

Haeri, S.M., Garakani, A., Khosravi, A. and Meehan, C.L. (2014), "Assessing the hydro-mechanical behavior of collapsible soils using a modified triaxial test device", *Geotech. Test. J.*, **37**(2), 190-204.

Haeri, S.M., Khosravi, A., Garakani, A.A. and Ghazizadeh, S. (2016), "Effect of soil structure and disturbance on hydromechanical behavior of collapsible loessial soils", *Int. J. Geomech.* [Online Publication]

He, Q.F. (2008), "Study on the mechanical and rheological properties of Yan'an Q_2 loess", Ph.D. Dissertation; Chang'an University, Xi'an, China.

Li, B.X. and Miao, T.D. (2009), "Research on water sensitivity of loess shear strength", *Chinese J. Rock Mech. Eng.*, **25**(5), 1003-1008.

Liang, Q.G., Li, J., Wu, X.Y. and Zhou, A.N. (2015), "Anisotropy of Q_2 loess in the Baijiapo tunnel on the Lanyu railway, China", *Bull. Eng. Geol. Environ.*, **75**(1), 109-124.

Luo, Y.D. (2011), "Research on shear strength of compacted soils considering saturation degree", *Rock and Soil Mechanics*, **32**(10), 3143-3148.

Luo, Y., Wang, T.H., Liu, X.J. and Zhang, H. (2014), "Laboratory study on shear strength of loess joint", *Arab. J. Sci. Eng.*, **39**(8), 7549-7554.

Muñoz-Castelblanco, J.A., Delage, P., Pereira, J.M. and Cui, Y.J. (2011), "Some aspects of the compression and collapse behaviour of an unsaturated natural loess", *Géotechnique Letters*, **1**(2), 17-22.

Muñoz-Castelblanco, J.A., Pereira, J.M., Delage, P. and Cui, Y.J. (2012), "The water retention properties of a natural unsaturated loess from Northern France", *Géotechnique*, **62**(2), 95-106.

Olson, R.E. (1998), "Settlement of embankments on soft clay", *J. Geotech. Geoenviron. Eng.*, **124**(8), 659-669.

Qian, Z.Z., Lu, X.L., Yang, W.Z. and Cui, Q. (2014), "Behaviour of micropiles in collapsible loess under tension or compression load", *Geomech. Eng., Int. J.*, **7**(5), 477-493.

Rahardjo, H., Meilani, I., Leong, E.C. and Rezaur, R.B. (2009), "Shear strength characteristics of a compacted soil under infiltration conditions", *Geomech. Eng., Int. J.*, **1**(1), 35-52.
Shen, C.N., Fang, X.W. and Wang, H.W. (2009), "Research on effects of suction, water content and dry density on shear strength of remolded unsaturated soils", *Rock Soil Mech.*, **30**(5), 1347-1352.
Tang, H., Dang, Q., Duan, Z., Zhao, F.S. and Song, F. (2014), "Study on creep characteristics of Q_2 loess of Xianyang area in the Guanzhong basin", *J. Disast. Prevent. Mitig. Eng.*, **34**(6), 758-763.
Vahedifard, F., Leshchinsky, D., Mortezaei, K. and Lu, N. (2016), "Effective stress-based limit-equilibrium analysis for homogeneous unsaturated slopes", *Int. J. Geomech.* [Online Publication]
Vilar, O.M. and Rodrigues, R.A. (2011), "Collapse behavior of soil in a Brazilian region affected by a rising water table", *Can. Geotech. J.*, **48**(2), 226-233.
Wang, L.H., Bai, X.H. and Feng, J.Q. (2010), "Discussion on shearing strength influencing factors of compacted loess-like backfill", *Chinese J. Geotech. Eng.*, **32**, 132-136.
Wang, J.J., Liang, Y., Zhang, H.P., Wu, Y. and Lin, X. (2014a), "A loess landslide induced by excavation and rainfall", *Landslides*, **11**(1), 141-152.
Wang, C.D., Zhou, S.H., Guo, P.J. and Wang, B.L. (2014b), "Experimental analysis on settlement controlling of geogrid-reinforced pile-supported embankments on collapsible loess in high-speed railway", *Int. J. Pave. Eng.*, **15**(9), 867-878.
Wang, X.L., Zhu, Y.P. and Huang, X.F. (2014c), "Field tests on deformation property of self-weight collapsible loess with large thickness", *Int. J. Geomech.*, **14**(3), 04014001.
Wu, W.J., Chen, W.W., Song, B.H., Feng, L.T. and Ye, W.L. (2012), "Experiment on the shear characteristics of undisturbed Q_2 loess in Lanzhou", *J. Lanzhou Univ.* (*Natural Sciences*), **48**(6), 21-25.
Zhang, F.Y., Wang, G.H., Kamai, T., Chen, W.W., Zhang, D.X. and Yang, J. (2013), "Undrained shear behavior of loess saturated with different concentrations of sodium chloride solution", *Eng. Geol.*, **155**(3), 69-79.
Zhuang, J.Q. and Peng, J.B. (2014), "A coupled slope cutting — A prolonged rainfall-induced loess landslide: a 17 October 2011 case study", *Bull. Eng. Geol. Environ.*, **73**(4), 997-1011.

CC